



## Structural and photoluminescence properties of Eu<sup>3+</sup> doped KMgBO<sub>3</sub> phosphors

B. Siva Kumar<sup>a</sup>, H. Umamahesvari<sup>b\*</sup>, K. Thyagarajan<sup>c1\*</sup>, P. Ankoji<sup>c2\*</sup>, B. Munisudhakar<sup>d</sup>

<sup>a</sup>Department of Physics, JNTUA College of Engineering Kalikiri, Constituent college of Jawaharlal Nehru Technological University Anantapur, Anantapuramu - 515 002, India

<sup>b</sup>Department of Physics, Sreenivasa Institute of Technology and Management Studies (Autonomous), Chittoor-517 127, Affiliated to Jawaharlal Nehru Technological University Anantapur, Ananthapuramu, India

<sup>c1&c2</sup>Department of Physics, JNTUA College of Engineering, Pulivendula, Constituent college of Jawaharlal Nehru Technological University Anantapur, Ananthapuramu-516 390, India

<sup>d</sup> Department of Physics, S V College of Engineering, Karakambadi Road, Tirupathi 517507, Affiliated to Jawaharlal Nehru Technological University Anantapur, Ananthapuramu, India

<sup>b\*</sup>E-mail: [umamaheswarihema@gmail.com](mailto:umamaheswarihema@gmail.com)

<sup>c1\*</sup>E-mail: [ktrjntu@gmail.com](mailto:ktrjntu@gmail.com)

<sup>c2\*</sup>E-mail: [ankphyl@gmail.com](mailto:ankphyl@gmail.com)

### Abstract

In order to develop red emitting phosphors for W-LEDs, a series of Eu<sup>3+</sup> (2, 4, 6 and 8 mol%) doped potassium magnesium borate (KMB) phosphors were prepared using a solid state reaction technique at 700 °C. The structure, morphology, optical and luminescent properties of prepared phosphors were investigated using X-ray diffraction (XRD), Fourier-transform infrared spectroscopy (FTIR), scanning electron microscope (SEM), absorption spectrometer (UV-Vis) and spectrofluorimeter. In accordance with the XRD analysis, the undoped and Eu<sup>3+</sup> doped phosphor samples have a single phase cubic crystal structure with P2<sub>1</sub>3 space group. Based on the FTIR studies, all of the synthesised phosphor samples have metallic and B-O bonds. The absorption bands in the UV-Vis-NIR region were identified and the energy band gap values were evaluated using the absorption spectra. The excitation spectra of Eu<sup>3+</sup> ions doped KMB phosphors were recorded at 617 nm emission wavelength and it consist of four excitation bands. From the excitation spectra, 398 nm is the most prominent excitation band among all the excitation bands, so this wavelength has been employed to obtain the emission spectra. Four emission bands were identified in emission spectra at 594, 617, 650 and 711 nm

corresponding to the electronic transitions of Eu<sup>3+</sup> ions  $^5D_0 \rightarrow ^7F_1$ ,  $^5D_0 \rightarrow ^7F_2$ ,  $^5D_0 \rightarrow ^7F_3$  and  $^5D_0 \rightarrow ^7F_4$ . The strong intense emission band was noticed at 617 nm among all these luminescence bands. The luminescence intensity enhanced up to 6 mol% with rising Eu<sup>3+</sup> ion concentration, furthermore activating ion concentration increased the luminescence was intensity decreased. This is attributing to the concentration-quenching effect. The CIE and CCT values were computed using luminescence spectra and the decay life time values of all Eu<sup>3+</sup> doped phosphor samples were estimated. All of these findings suggest that the prepared KMB: Eu<sup>3+</sup> red light emitting phosphor materials are appropriate for white light emitting diode and display applications.

**Keywords:** Solid-state reaction; Rare earth ion; Emission analysis; CIE; KMgBO<sub>3</sub> phosphor.

## 1. Introduction

Rare earth (RE) doped phosphor materials are commonly used in lighting, display devices, storage devices, medical instruments and a variety of other applications [1, 2]. Aside from the various applications of RE doped phosphors, the lighting and display industries are focused on developing efficient high intensity white light emitting diodes (WLEDs) due to their advantages in terms of high brightness, reliability, long lifetime, low environmental impact and energy savings [3]. The WLEDs are expected to replace conventional incandescent and fluorescent lamps in the near future. Basically the white light is composed of many colours and the LED produce monochromatic colours, hence it is a considerable challenge for LED technology [4, 5]. The commercial WLEDs are produced by three systems such that, red, green and blue (RGB) combined LED, RGB phosphor coated UV light emitted LED and yellow phosphor coated blue colour emitted LED [6, 7]. The commercially used red phosphor Y<sub>2</sub>O<sub>2</sub>S:Eu<sup>3+</sup> has lower efficiency than blue and green phosphors and is unstable due to sulphide gas release [8]. Despite having a high luminous efficiency, the WLED still has a low CRI due

to a lack of red light [9]. As a result, more efficient red or orange red emitting phosphors required for WLED fabrication. Hence it is essential to find novel red or orange-red light emitting phosphors with stable host materials, it exhibits prominent absorption and emission under ~400 nm excitation. Recently researchers have been concentrated to develop the novel orange-red materials for use in white LEDs [10].

Rare earth oxides (RE<sub>2</sub>O<sub>3</sub>) are the most stable elements, in which the rare earth ions hold typically a trivalent state [11]. Because of the optical, electronic and chemical properties deriving from their 4f electrons, the rare earth oxides have been extensively utilized in the areas of luminescent devices, optical transmission, bio-chemical probes and medical diagnosis [12, 13]. In addition the RE doped inorganic compounds are utilized in several applications. The luminescence properties of Eu<sup>3+</sup> ions are due to intra 4f<sup>6</sup> (4f-4f) transition mechanisms between the excited and ground states [14]. Because the 4f shell is shielded by the outer filled 5s and 5p shells, the emission wavelength of the Eu<sup>3+</sup> ion 4f-4f transition is relatively insensitive to host and temperature. Currently, transitions of Eu<sup>3+</sup> ions are acquiring attention can improve the colour temperatures and colour rendering index (CRI) of white light emitting diodes [15]. The improvement in the lighting efficiency of WLEDs is strongly reliant on the advancement of phosphor materials.

Generally borate compound substances have well thermally and chemically stable with the rigid crystal nature of the closely bonded 3-dimensional matrix, it has been attracting significant attention for light-emitting utilisations [16]. RE activated borate phosphors possess high attention by dint of their utility of synthesis at low temperature and good near ultraviolet (NUV) transmittance characteristics. Recently researchers investigated various RE doped borate materials, like as Tm<sup>3+</sup> activated Sr<sub>2</sub>B<sub>2</sub>O<sub>5</sub> [17] and Ce<sup>3+</sup> activated NaSrBO<sub>3</sub> [18] are for blue luminescence, Tb<sup>3+</sup> activated Sr<sub>2</sub>B<sub>2</sub>O<sub>5</sub> [19] and Ce<sup>3+</sup> activated NaBaBO<sub>3</sub> [20] are for

green emission, LiSr<sub>4</sub>(BO<sub>3</sub>)<sub>3</sub> doped with Sm<sup>3+</sup> [21] and CaB<sub>2</sub>O<sub>4</sub> [22] doped with Eu<sup>3+</sup> are for red emitting material. In 2010, the crystal nature of a novel borate KMgBO<sub>3</sub> was firstly reported by Wu et al. [23], and then RE free Mn<sup>2+</sup> doped KMgBO<sub>3</sub> was reported in 2014 [24]. Based on literature survey, no reports on structural nature, optical properties and photoluminescence characteristics of Eu<sup>3+</sup> ions activated KMgBO<sub>3</sub> (KMB) phosphor material.

This paper describes the preparation, structural nature, optical properties and emission characteristics of Eu<sup>3+</sup> activated KMgBO<sub>3</sub> phosphors made using a solid state technique. The structural, morphological, optical, emission, excitation and decay life time characteristics of the prepared phosphors were thoroughly investigated.

## 2. Experimental

### 2.1. Sample synthesis

The KMgBO<sub>3</sub>: xEu<sup>3+</sup> phosphors (x= 0, 2, 4, 6 and 8 mol%) were synthesised using the solid state technique. High-purity powders of H<sub>3</sub>BO<sub>3</sub>, MgO, K<sub>2</sub>CO<sub>3</sub> and Eu<sub>2</sub>O<sub>3</sub> were used as starting materials without further purification. Based on the stoichiometric relation, the corresponding initial materials were weighed then mixed, and a small amount of acetone was added before crushing in an agate mortar for 60 minutes to obtain uniformity. Which were sintered in a porcelain crucible at a temperature of 200 °C for 120 minutes. After that, the phosphor powders were ground again for 30 minutes and placed in a porcelain crucible heated at 700 °C with the help of a muffle furnace for 5 hours. Then being slowly cooled to laboratory temperature and the samples were examined.

The XRD profiles for the KMB: xEu<sup>3+</sup> (x = 0, 2, 4, 6 and 8 mol%) series were obtained using a Shimadzu XRD-6000 diffractometer in the Bragg-Brentano geometry. This instrument was outfitted with a Cu<sub>α</sub> X-ray source, a scintillation counter as a detector, and a Ni filter to eliminate K<sub>β</sub> radiation. The FTIR spectrometer Shimadzu tracer-100 with ATR Diamond

accessories was used to obtain the IR spectrum of phosphors in the 500-4000 cm<sup>-1</sup> range. A scanning electron microscope was used to measure the phosphor surface study investigation (SEM, S-4800). The diffusion reflectance spectra were taken using a UV-Vis-NIR Spectrophotometer (Varian: 5000). The decay curves, excitation and emission spectra were recorded using a fluorescence spectrometer (EDIN-BURGH FLS980) equipped with a 450 W xenon lamp.

### 3. Results and discussion

#### 3.1. Crystal structure

The XRD pattern of solid state synthesised KMB: xEu<sup>3+</sup> (x= 0, 2, 4, 6 and 8 mol%) phosphors is shown in Fig. 1, the diffraction bands are similar to the ICSD no. 174336 without any supplementary peaks. This result confirmed that the current phosphors are single phased, pure cubic crystals with the P2<sub>1</sub>3 space group and lattice constant a = b = c = 6.8344 [24]. All the diffraction peaks were indexed with miller indices. Eq.1 [25] gives the mean crystallite size (D) derived from the Debye-Scherer's relation.

$$D_{hkl} = k\lambda / [\beta(2\theta) \cos\theta] \quad (1)$$

where  $\lambda$ : X-ray wavelength (1.5405 Å), k: constant (0.9),  $\beta$ : full-width at half maximum (FWHM, in radian) and  $\theta$ : diffraction angle of an observed profile. The prominent diffraction peak at (0 1 2) was utilised to obtain the D values of the KMB: xEu<sup>3+</sup> (x= 0, 2, 4, 6 and 8 mol%) phosphors and were identified to be 1.146, 1.135, 1.120, 1.021 and 0.982  $\mu\text{m}$ , respectively.

#### 3.2. FTIR study

FTIR exhibits molecule vibration characteristics due to infrared wavelength (IR) absorption. The absorption intensity indicates how sharply the absorption energy can be exchanged to molecules, causing the molecule dipole moment to change and causing molecule vibrations. Fig. 2 exhibits the FTIR spectra of the KMB: xEu<sup>3+</sup> (x= 0, 2, 4, 6 and 8 mol%)

phosphors. By this spectra the absorption bands observed at 2900-3700 cm<sup>-1</sup> assigned to –OH molecule stretching vibrations, these bands were owing to materials are absorbing surrounding water contents [26]. 1663 cm<sup>-1</sup> absorption band was identified to asymmetric stretching B-O bonds bending vibration. 1305 cm<sup>-1</sup> absorption band was observed and it belongs to B-O asymmetric stretching vibrations. 1004 and 856 cm<sup>-1</sup> absorption bands were noticed and its corresponding to B-O bending vibrations of trigonal BO<sub>3</sub>. At absorption peak 703 cm<sup>-1</sup> absorption bands were identified and these are belongs to Mg/K–O stretching vibrations of Mg/KO<sub>6</sub> Octahedron [27] FTIR spectra confirm the presence of B-O of trigonal BO<sub>3</sub> and metallic bonds in KMB.

### 3.3. Morphological studies

SEM images of KMB: xEu<sup>3+</sup> (x= 2, 4, 6 and 8 mol%) phosphor material are shown in Fig. 3(a-d). It indicates the irregular morphological structures as grinding of the materials while preparing and high temperatures used for making the phosphor material. From all the images was observed in sizes of the particles varied from 1 to 3 μm.

### 3.4. Diffuse reflectance studies

DRS spectra of KMB: xEu<sup>3+</sup> (x= 2, 4, 6 and 8 mol%) phosphors are shown Fig. 4. According to the absorption spectra, prominent absorption peaks at 259, 387 and 1451 nm were caused by electron passage from a valence band to a conduction band. Besides, as the concentration of Eu<sup>3+</sup> ions increased, the absorption peaks slightly shifted towards the lower wavelength (blue shift). There were no weak absorption peaks observed in any of the samples in the UV-Vis region, indicating that surface defects, traps, and impurities are very low. The optical energy gap (E<sub>g</sub>) for the KMB: xEu<sup>3+</sup> (x= 2, 4, 6, and 8 mol%) phosphors was calculated using wood and Tauc's relation. The E<sub>g</sub> is a combination of photon energy and absorbance, as defined by Eq. 2 [28].

$$h\nu\alpha \propto (h\nu - E_g)^k \quad (2)$$

where  $h$ : Planck's constant,  $\nu$ : frequency,  $E_g$ : optical energy gap,  $\alpha$ : absorbance and  $k$ : constant combined to various class of electronic transitions ( $k=1/2, 2, 3/2$  and  $3$ ). From the literature that oxide materials have direct allowed electronic transitions,  $k=1/2$  was employed in standard Eq. 2 as a result, the  $E_g$  values were estimated by extrapolating the straight line of the tail or the curve  $(h\nu\alpha)^2 = 0$  in an absorption spectrum, as shown in Fig. 5. The  $E_g$  values for KMB: xEu<sup>3+</sup> ( $x= 2, 4, 6,$  and  $8$  mol%) phosphors estimated from this graph were 4.19, 4.10, 4.01, and 3.75 eV, respectively. Energy gap values were decreased as Dy<sup>3+</sup> concentration increased due to structural defects such as vacancies and the degree of structural order disorder in the crystal, which is capable of exchanging the intermediate energy level allocation within in the band gap.

### 3.5. Photoluminescence studies

The excitation spectra monitored under 617 nm emission wavelength of the KMB: xEu<sup>3+</sup> ( $x= 2, 4, 6$  and  $8$  mol %) phosphors are depicted in Fig. 6. It has excitation peaks at 306, 363, 398 and 467 nm that are attributed to intra 4f-shell electronic transitions of Eu<sup>3+</sup> ions from the <sup>7</sup>F<sub>0</sub> ground-state and thermally populated lowest-lying <sup>5</sup>H<sub>6</sub>, <sup>5</sup>D<sub>4</sub>, <sup>5</sup>L<sub>6</sub>, and <sup>5</sup>D<sub>2</sub> states, respectively. When compared to other absorption peaks, the band at 398 nm is the prominent one, which corresponds well to the emission of commercial N-UV chips, exhibited a relatively high intensity, indicating that the samples studied can be excited by N-UV light.

The emission spectra recorded under 398 nm excitation wavelength of the KMB: xEu<sup>3+</sup> ( $x= 2, 4, 6$  and  $8$  mol %) phosphors are depicted in Fig. 7. The emission spectra has intense red emission centered at 617 nm originates from the <sup>5</sup>D<sub>0</sub> → <sup>7</sup>F<sub>2</sub> transition and it is dominant in the luminescence spectrum, which is an advantage for obtaining red phosphor of high color purity. Other weaker emission bands at were identified in emission spectra at 594, 650 and 711 nm corresponding to the electronic transitions of Eu<sup>3+</sup> ions <sup>5</sup>D<sub>0</sub>→<sup>7</sup>F<sub>1</sub>, <sup>5</sup>D<sub>0</sub>→<sup>7</sup>F<sub>3</sub> and <sup>5</sup>D<sub>0</sub>→<sup>7</sup>F<sub>4</sub>, respectively. The Eu<sup>3+</sup> ions are known as structural markers, this is because they exhibit two spectrally adjacent emissions: one falling in the yellow spectral range and related to the <sup>5</sup>D<sub>0</sub> →

<sup>7</sup>F<sub>1</sub> transition, is of purely magnetic dipole (MD) nature (according to the selection rule  $\Delta J = 0, \pm 1$ , except of  $0 \rightarrow 0'$ ) and its probability is almost unchanged with respect to the host matrix and another falling in the red spectral range and related to the <sup>5</sup>D<sub>0</sub> → <sup>7</sup>F<sub>2</sub> transition, is purely electric dipole (ED) and it is rather sensitive to the local symmetry of the rare-earth site and its distortion (a hypersensitive transition). In general, when Eu<sup>3+</sup> ions are located in sites without inversion symmetry, the red emission from the <sup>5</sup>D<sub>0</sub> → <sup>7</sup>F<sub>2</sub> ED transition dominates in the PL spectrum, whereas the yellow emission originating from the <sup>5</sup>D<sub>0</sub> → <sup>7</sup>F<sub>1</sub> MD transition becomes dominant when Eu<sup>3+</sup> ions occupy sites with inversion symmetry [29]. For KMB: xEu<sup>3+</sup> phosphors, the ED transition is dominant, suggesting that Eu<sup>3+</sup> ions reside in sites without inversion symmetry, which agrees with the structural analysis (C<sub>3</sub> and C<sub>s</sub> site symmetries). Based on the Eu<sup>3+</sup> ion concentration variance of the luminescence intensity, initially enhances and attains a maximum at x = 6 mol% and further deflation owing to the concentration quenching influence. The concentration quenching is originated by the progress of non-radiative energy transfer among surrounding Eu<sup>3+</sup> ions if the activating concentration reaches a critical value [30, 31].

### 3.6. Emission decay

Fig. 8 represents the emission decay curves of KMB: xEu<sup>3+</sup> (x = 2, 4, 6 and 8 mol%) phosphors samples. The luminescence was observed at 617 nm (decay from the metastable excited state <sup>5</sup>D<sub>0</sub>). The decay curves are purely double exponential for all the investigated samples. This suggests that the existing of Eu<sup>3+</sup> ions in two discrete crystallographic positions with different coordination and symmetry. The decay lifetime of all the prepared samples have estimated, and were found to be 1.20, 1.05, 0.69 and 0.65 ms for KMB: xEu<sup>3+</sup> (x = 2, 4, 6 and 8 mol%) phosphors, respectively. With the enhancing of the Eu<sup>3+</sup> activating level in KMB, the

length among the dopant ions deflation caused to enhancing cross-relaxation probability, which decreases the decay lifetime.

### 3.7. Chromaticity coordinates and CCT

Fig. 9 illustrates the CIE (Commission International de l'Eclairage) 1931 colour coordinates (x, y) of emission of the KMB: xEu<sup>3+</sup> (x= 2, 4, 6 and 8 mol%) phosphors. The (x, y) coordinates were estimated from the PL spectra and their values are computed in Table 1. The prominent luminescence intensity (x = 6 mol%), the chromaticity coordinates are (0.6445, 0.3515) assigning to a predominant wavelength of 617 nm falling in the red colour region.

Table 1. CIE and CCT values of KMB: xEu<sup>3+</sup> (x= 2, 4, 6 and 8 mol%) phosphors.

Sample	CIE (x, y)	CCT (K)
KMB: 2 mol% Eu <sup>3+</sup>	(0.6413, 0.3556)	1087
KMB: 4 mol% Eu <sup>3+</sup>	(0.6426, 0.3545)	1077
KMB: 6 mol% Eu <sup>3+</sup>	(0.6445, 0.3515)	1058
KMB: 8 mol% Eu <sup>3+</sup>	(0.6433, 0.3531)	1069

The correlated colour temperature (CCT) was determined using the McCamy's empirical formula:

$$\text{CCT} = -437 n^3 + 3601 n^2 - 6861 n + 5514.31 \quad (3)$$

Where  $n = (x-x_e)/(y-y_e)$  and  $x_e = 0.332$ ,  $y_e = 0.186$  are the coordinates of the epicentre of convergence. The determined values of CCT are listed in Table 1. The prominent luminescence intensity (x = 6 mol%), the CCT value 1058 K. This is indicated that the emitted light is warm light.

### 4. Conclusions

The traditional solid-state reaction technique used to synthesized the novel single-phase red light emitting KMB: xEu<sup>3+</sup> (x= 0, 2, 4, 6 and 8 mol%) phosphors. A systematic

investigation of the crystal structure, morphology, molecular vibrations, optical and luminescent characteristics of the prepared phosphors was accomplished. The XRD prompted that all the prepared phosphors crystallize in the cubic system with P2<sub>1</sub>3 space group without any additional peaks. This is suggested that the prepared all the samples are in single phase without any impurity elements. The FTIR studies confirmed that all the prepared samples having B-O of trigonal BO<sub>3</sub>, B-O-B linkages and metallic bonds. The optical energy band gap values were estimated by using absorption spectra. The emission spectra recorded under 398 nm, the emission bands were observed at 594, 617, 650 and 711 nm corresponding to the electronic transitions of Eu<sup>3+</sup> ions <sup>5</sup>D<sub>0</sub>→<sup>7</sup>F<sub>1</sub>, <sup>5</sup>D<sub>0</sub>→<sup>7</sup>F<sub>2</sub>, <sup>5</sup>D<sub>0</sub>→<sup>7</sup>F<sub>3</sub> and <sup>5</sup>D<sub>0</sub>→<sup>7</sup>F<sub>4</sub>, respectively. Among all these emission bands the prominent emission band observed at 617 nm. The emission intensity enhanced with the rise of Eu<sup>3+</sup> ion concentration up to 6 mol%, further enhancement of doping concentration the emission intensity is decreased which is due to concentration quenching effect. The CIE and CCT values were evaluated from emission spectra, which were confirmed that the emitted light in red coloured warm light. The decay life time values were estimated for all Eu<sup>3+</sup> doped phosphors samples. All these results recommend that the present prepared phosphor samples are well suitable for red component in white light emitting diode and display applications.

## References

- [1] I.P. Sahu, D.P. Bisen, N. Brahme, Structural characterization and optical properties of Ca<sub>2</sub>MgSi<sub>2</sub>O<sub>7</sub>:Eu<sup>2+</sup>, Dy<sup>3+</sup> phosphor by solid state reaction method, *J. Biol. Chem. Lumin.* 30 (2015) 526-532.
- [2] F.W. Kang, Y. Hu, L. Chen, X.J. Wang, H. Wu, Z. Mu, Luminescent properties of Eu<sup>3+</sup> in MWO<sub>4</sub> (M=Ca, Sr, Ba) matrix, *J. Lumin.* 135 (2013) 113-119.
- [3] V. Vitola, D. Millers, I. Bite, K. Smits, A. Spustaka, Recent progress in understanding the persistent luminescence in SrAl<sub>2</sub>O<sub>4</sub>: Eu, Dy, *Mater. Sci. Technol.* 35 (2019) 1661-1677
- [4] H.W. Leverenz, *An Introduction to Luminescence of Solids*, Dover Publications Inc., New York, 1968.

- [5] Z. Wang, S. Lou, P. Li, Enhanced orange-red emission of Sr<sub>3</sub>La(PO<sub>4</sub>)<sub>3</sub>:Ce<sup>3+</sup>, Mn<sup>2+</sup> via energy transfer, *J. Lumin.* 156 (2014) 87-90.
- [6] J. Liu, K. Liang, Z.C. Wu, Y.M. Mei, S.P. Kuang, D.X. Li, The reduction of Eu<sup>3+</sup> to Eu<sup>2+</sup> in a new orange-red emission Sr<sub>3</sub>P<sub>4</sub>O<sub>13</sub>:Eu phosphor prepared in air and its photoluminescence properties, *Ceram. Int.* 40 (2014) 8827-8831.
- [7] P. Ankoji, B.H. Rudramadevi, structural and luminescence properties of Eu<sup>3+</sup> doped LaAlO<sub>3</sub> nanophosphors by hydrothermal method, *J. Mater. Sci.: Mater. in Electro.*, 30 (2019) 2750-2762.
- [8] Y. Chen, X. Cheng, M. Liu, Z. Qi, C. Shi, Comparison study of the luminescent properties of the white light long afterglow phosphors: Ca<sub>x</sub>MgSi<sub>2</sub>O<sub>5+x</sub>:Dy<sup>3+</sup> (x= 1, 2, 3), *J. Lumin* 129 (2009) 531-535.
- [9] M. Xu, L. Wang, L. Liu, D. Jia, R. Sheng, Influence of Gd<sup>3+</sup> doping on the luminescent of Sr<sub>2</sub>P<sub>2</sub>O<sub>7</sub>:Eu<sup>3+</sup> orange-red phosphors, *J. Lumin.* 146 (2014) 475-479.
- [10] X.M. Zhang, F.G. Meng, C. Yang, H.J. Seo, Temperature dependence of luminescence properties of Sr<sub>3</sub>P<sub>4</sub>O<sub>13</sub>: Eu<sup>2+</sup> polycrystalline ceramics, *J. Lumin.* 140 (2013) 74-77.
- [11] Z. Song, J. Liao, X. Ding, T. Zhou, Q.L. Liu, Stability of divalent/trivalent oxidation state of europium in some Sr-based inorganic compounds, *J. Lumin.* 132 (2012) 1768-1773.
- [12] T.W. Kuo, T.M. Chen, Synthesis and luminescence of Ca<sub>4</sub>YO(BO<sub>3</sub>)<sub>3</sub>:Eu<sup>3+</sup> for fluorescent lamp application, *Opt. Mater.* 32 (2010) 882-885.
- [13] H. Wu, Y. Hu, G. Ju, L. Chen, X. Wang, Z. Yang, Photoluminescence and thermoluminescence of Ce<sup>3+</sup> and Eu<sup>2+</sup> in Ca<sub>2</sub>Al<sub>2</sub>SiO<sub>7</sub> matrix, *J. Lumin.* 131 (2011) 2441-2445.
- [14] H. Wu, Y. Hu, L. Chen, X. Wang, Investigation on the enhancement and the suppression of persistent luminescence of Re<sup>3+</sup> doped Sr<sub>2</sub>EuMgSi<sub>2</sub>O<sub>7</sub> (Re= Dy, Yb), *J. Alloys Compd.* 509 (2011) 4304-4307.
- [15] I.P. Sahu, D.P. Bisen, N. Brahme, L. Wanjari, R.K. Tamrakar, Structural characterization and luminescence properties of bluish-green emitting SrCaMgSi<sub>2</sub>O<sub>7</sub>:Eu<sup>2+</sup>, Dy<sup>3+</sup> phosphor by solid state reaction method, *Res. Chem. Intermed.* 41 (11) (2015) 8797-8814.
- [16] Z. Zhang, A. Song, X. Shen, Q. Lian, X. Zheng, A novel white emission in Ba<sub>10</sub>F<sub>2</sub>(PO<sub>4</sub>)<sub>6</sub>:Dy<sup>3+</sup> single-phase full-color phosphor, *Mater. Chem. Phys.* 151 (2015) 345-350.
- [17] L. Cai, L. Ying, J. Zheng, B. Fan, R. Chen, C. Chen, Luminescent properties of Sr<sub>2</sub>B<sub>2</sub>O<sub>5</sub>: Tm<sup>3+</sup>, Na<sup>+</sup> blue phosphor, *Ceram. Int.* 40 (2014) 6913-6918.

- [18] W.R. Liu, C.-H. Huang, C.-P. Wu, Y.-C. Chiu, Y.-T. Yeh, T.-M. Chen, High efficiency and high color purity blue-emitting NaSrBO<sub>3</sub>:Ce<sup>3+</sup> phosphor for near UV light-emitting diodes, *J. Mater. Chem.* 21 (2011) 6869-6874.
- [19] R. Wang, J. Xu, C. Chen, Luminescent characteristics of Sr<sub>2</sub>B<sub>2</sub>O<sub>5</sub>: Tb<sup>3+</sup>, Li<sup>+</sup> green phosphor, *Mater. Lett.* 68 (2012) 307-309.
- [20] R. Yu, N. Xue, H. Li, H. Ma, Synthesis, structure, and peculiar green-emitting of NaBaBO<sub>3</sub>: Ce<sup>3+</sup> phosphor, *Dalton Trans.* 43 (2014) 10969-10976.
- [21] Z.-W. Zhang, Y.-S. Peng, X.-H. Shen, J.-P. Zhang, S.-T. Song, Q. Lian, Enhanced novel orange red emission in LiSr<sub>4-x</sub>(BO<sub>3</sub>)<sub>3</sub>: xSm<sup>3+</sup> by K<sup>+</sup>, *J. Mater. Sci.* 49 (2014) 2534-2541.
- [22] J. Huang, L. Zhou, Q. Pang, F. Gong, J. Sun, W. Wang, Photoluminescence properties of a novel phosphor CaB<sub>2</sub>O<sub>4</sub>:Eu<sup>3+</sup> under NUV excitation, *Luminescence* 24 (2009) 363-366.
- [23] L. Wu, J.C. Sun, Y. Zhang, S.F. Jin, Y.F. Kong, J.J. Xu, Structure determination and relative properties of novel chiral orthoborate KMgBO<sub>3</sub>, *Inorg. Chem.* 49 (2010) 2715-2720.
- [24] L. Wu, B. Wang, Y. Zhang, L. Li, H.R. Wang, H. Yi, Y.F. Kong, J.J. Xu, Structure and photoluminescence properties of a rare-earth free red-emitting Mn<sup>2+</sup>-activated KMgBO<sub>3</sub>, *Dalton Trans.* 43 (2014) 13845-13851.
- [25] P. Ankoji, B.H. Rudramadevi, structural and luminescence properties of LaAlO<sub>3</sub>:Sm<sup>3+</sup> nanophosphors synthesized via hydrothermal method, *Opt. Mater.*, 95 (2019) 109249-109257.
- [26] L.J.Q. Maia, A. Ibanez, L. Ortega, V.R. Mastelaro, A.C. Hernandez, Er:YAB nanoparticles and vitreous thin films by the polymeric precursor method, *J. Nanopart. Res.* 10 (2008) 1251-1262.
- [27] E. Beregi, A. Watterich, L. Kovacs, J. Madarasz, Solid-state reactions in Y<sub>2</sub>O<sub>3</sub>:3Al<sub>2</sub>O<sub>3</sub>:4B<sub>2</sub>O<sub>3</sub> system studied by FTIR spectroscopy and X-ray diffraction, *Vib. Spectrosc.* 22 (2000) 169-173.
- [28] M. Jiao, C. Yang, M. Liu, Q. Xu, Y. Yu, H. You, Mo<sup>6+</sup> substitution induced band structure regulation and efficient near-UV-excited red emission in NaLaMg (W, Mo)O<sub>6</sub>:Eu phosphor, *Opt. Mater. Express* 7 (2017) 2660-2671.
- [29] J. Zhong, D. Chen, H. Xu, W. Zhao, J. Sun, Z. Ji, Red-emitting CaLa<sub>4</sub>(SiO<sub>4</sub>)<sub>3</sub>O:Eu<sup>3+</sup> phosphor with superior thermal stability and high quantum efficiency for warm w-LEDs, *J. Alloys Compd.* 695 (2017) 311-318.

- [30] Z. Ci, R. Guan, L. Jin, L. Han, J. Zhang, J. Ma, Y. Wang, Host-sensitized white light emitting phosphor MgY<sub>4</sub>Si<sub>3</sub>O<sub>13</sub>:Dy<sup>3+</sup> with satisfactory thermal properties for UV-LEDs, *Cryst. Eng. Comm.* 17 (2015) 4982–4986.
- [31] G. Zhu, S. Xin, A novel blue light pumped yellow-emitting phosphor RbZnPO<sub>4</sub>:Dy<sup>3+</sup> with satisfactory color tuning and thermal properties for high power warm white light emitting diodes, *RSC Adv.* 5 (2015) 10679–106799.

## Graphs

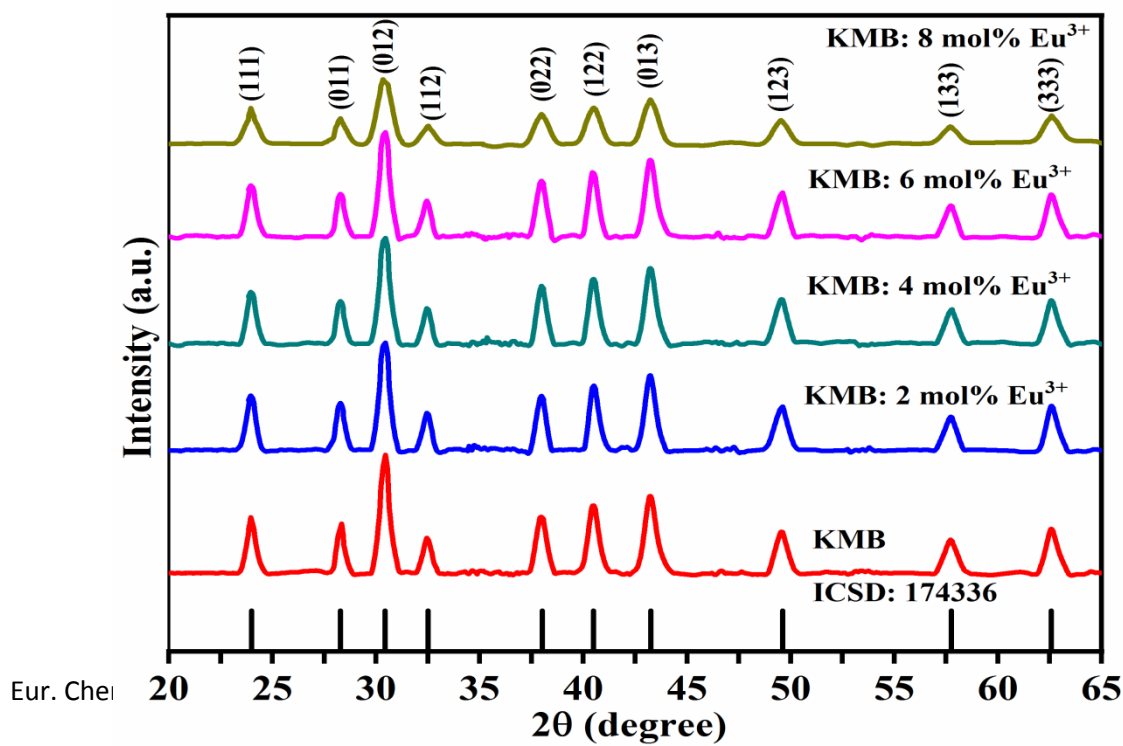


Fig.1. XRD spectra of  $\text{KMB: xEu}^{3+}$  ( $x=0, 2, 4, 6$  and  $8$  mol%) phosphors.

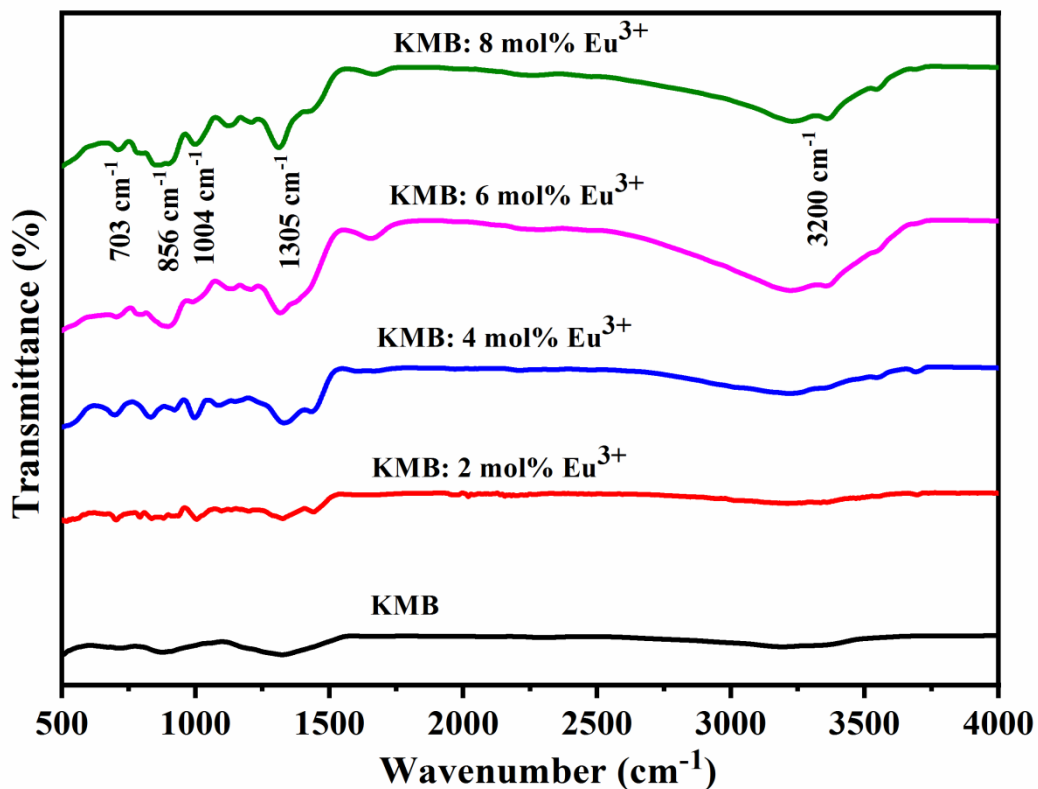


Fig. 2. FTIR spectra of  $\text{KMB: xEu}^{3+}$  ( $x=0, 2, 4, 6$  and  $8$  mol%) phosphors.

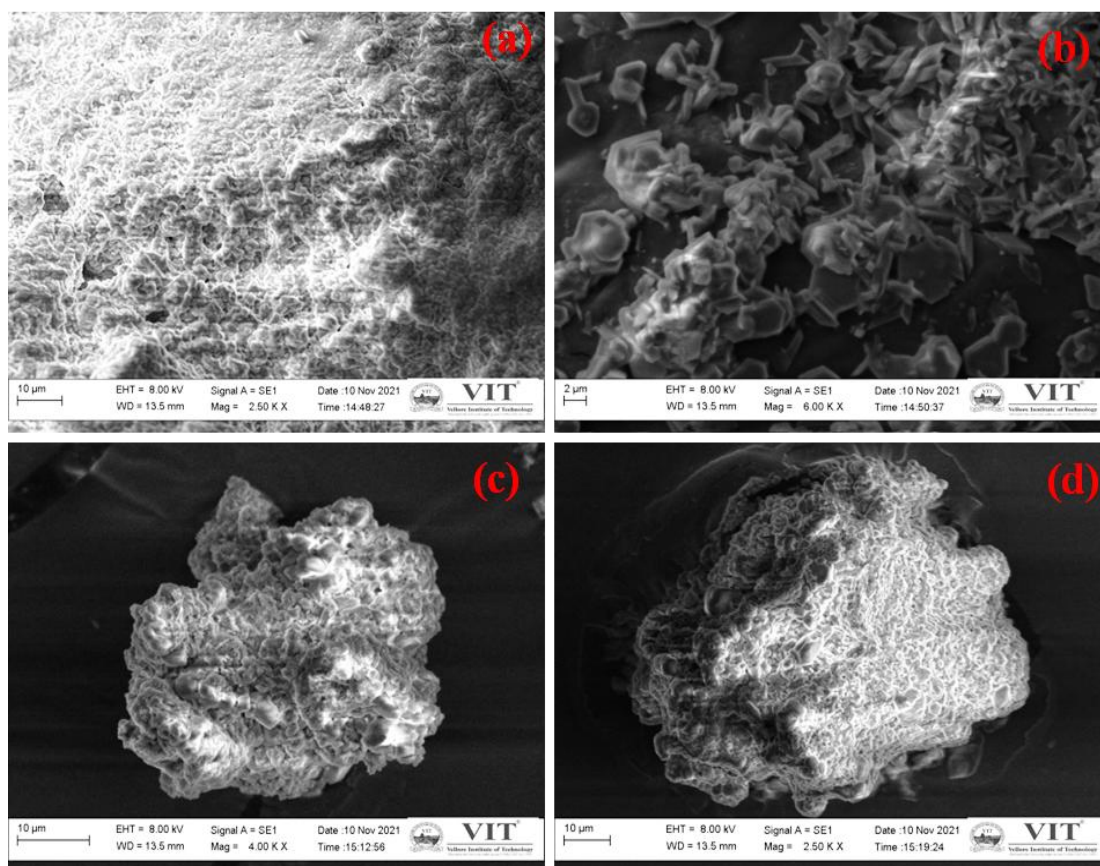


Fig. 3 (a-d). SEM images of  $\text{KMB: xEu}^{3+}$  ( $x = 2, 4, 6$  and  $8$  mol%) phosphors.

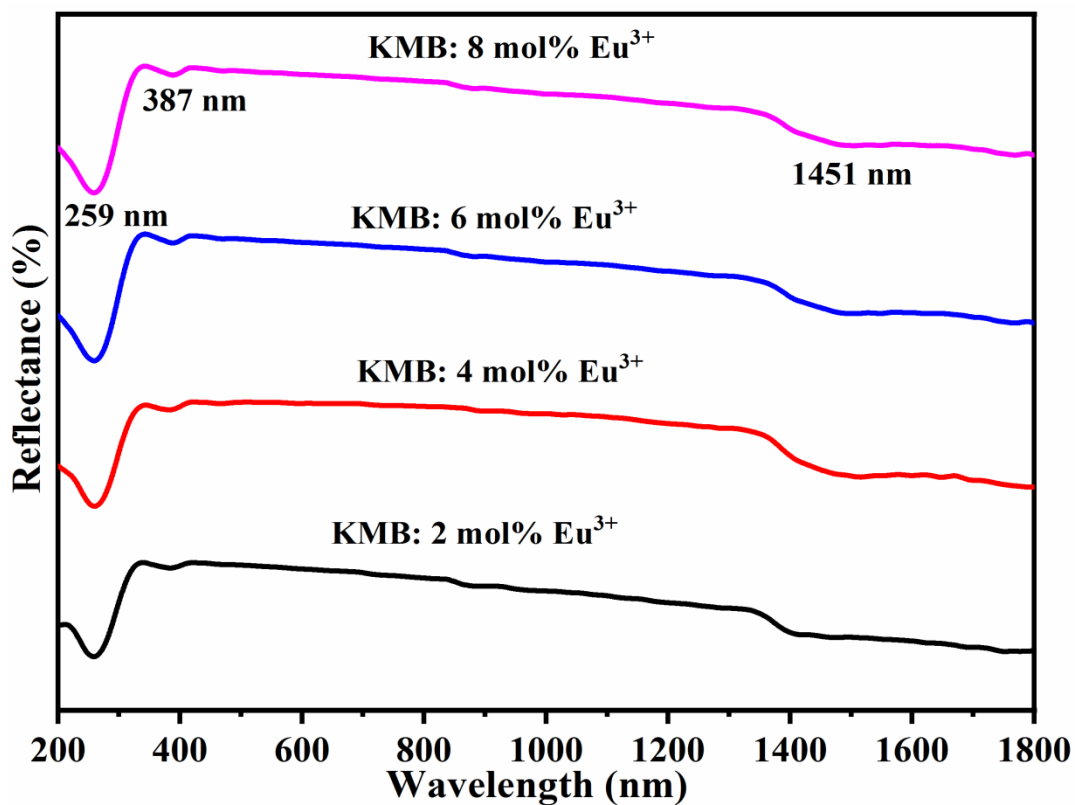


Fig. 4. Absorption spectra of KMB: xEu<sup>3+</sup> (x= 2, 4, 6 and 8 mol%) phosphors.

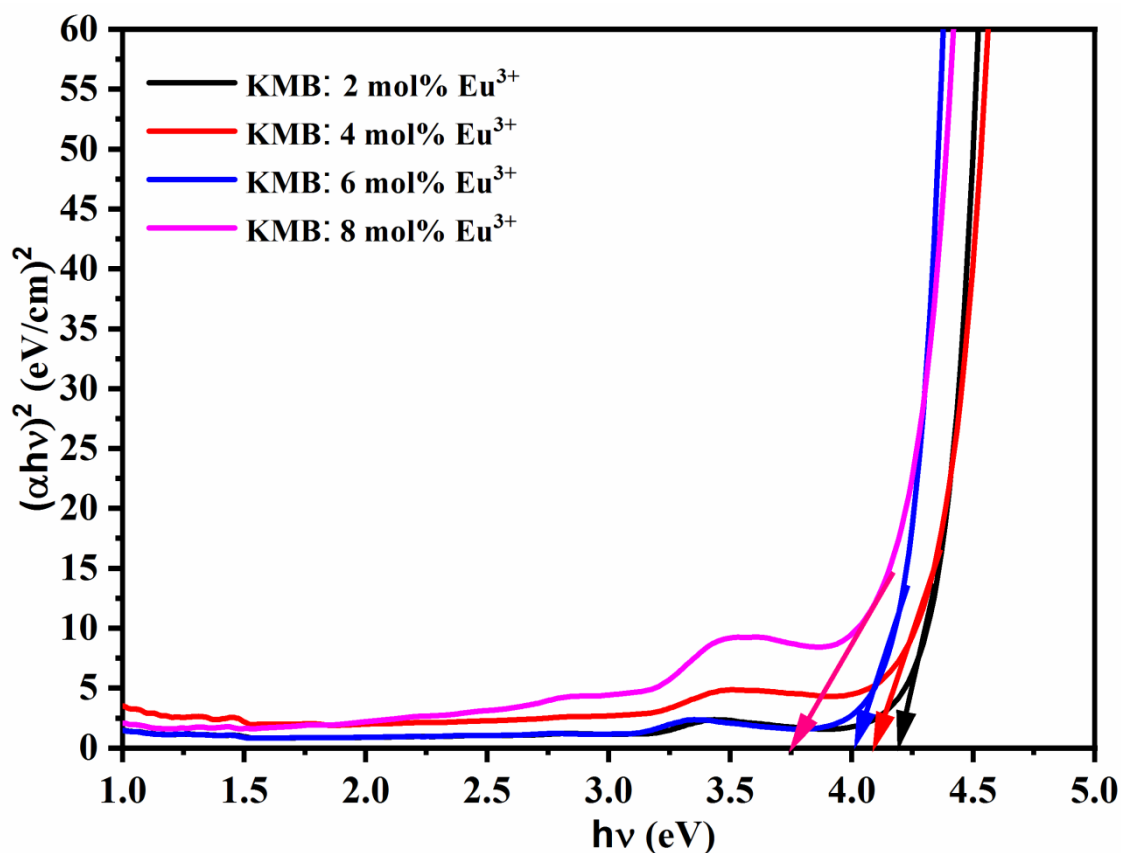


Fig. 5. Tauc's plot of KMB: xEu<sup>3+</sup> (x= 2, 4, 6 and 8 mol%) phosphors.

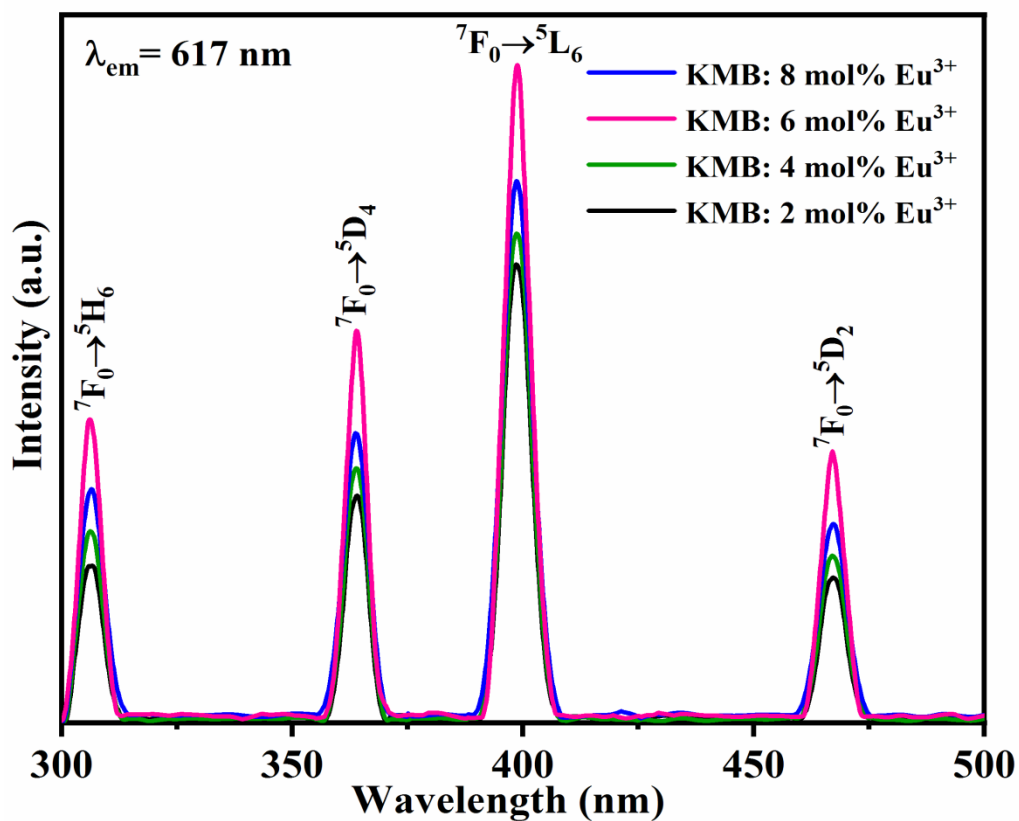


Fig. 6. Excitation spectra of  $\text{KMB}: x\text{Eu}^{3+}$  ( $x=2, 4, 6$  and  $8$  mol%) phosphors.

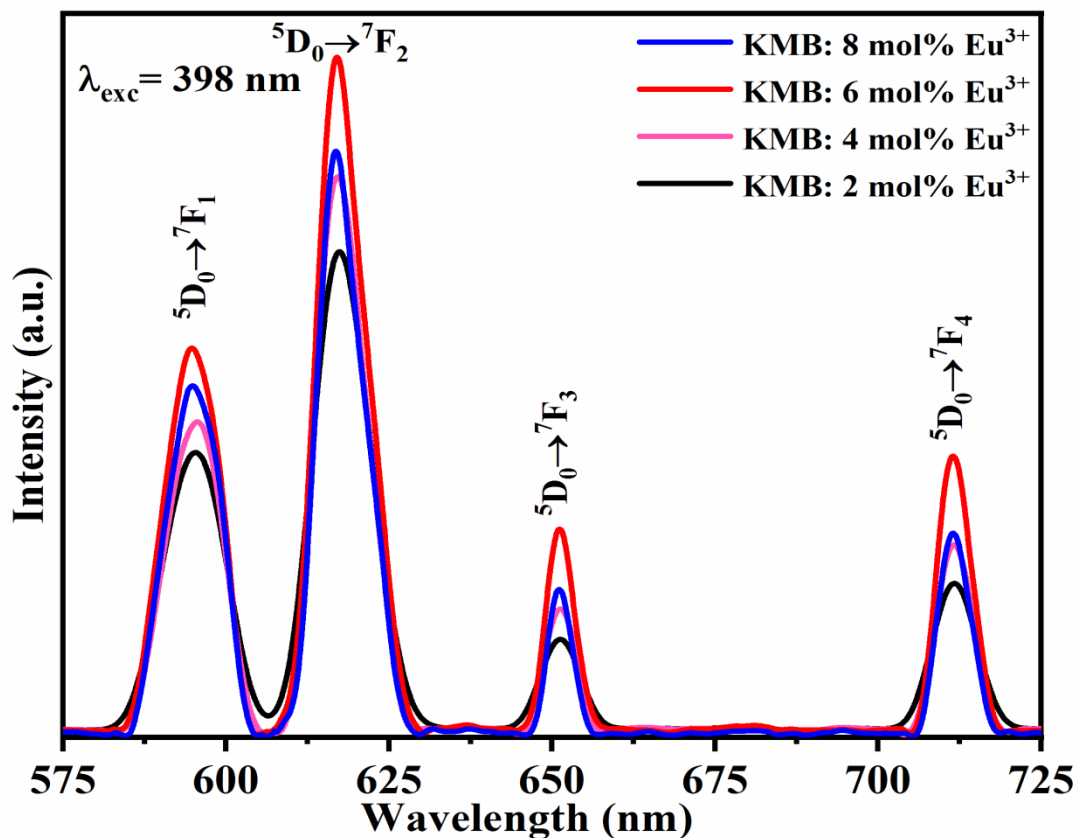


Fig. 7. Emission spectra of  $\text{KMB}: x\text{Eu}^{3+}$  ( $x=2, 4, 6$  and  $8$  mol%) phosphors.

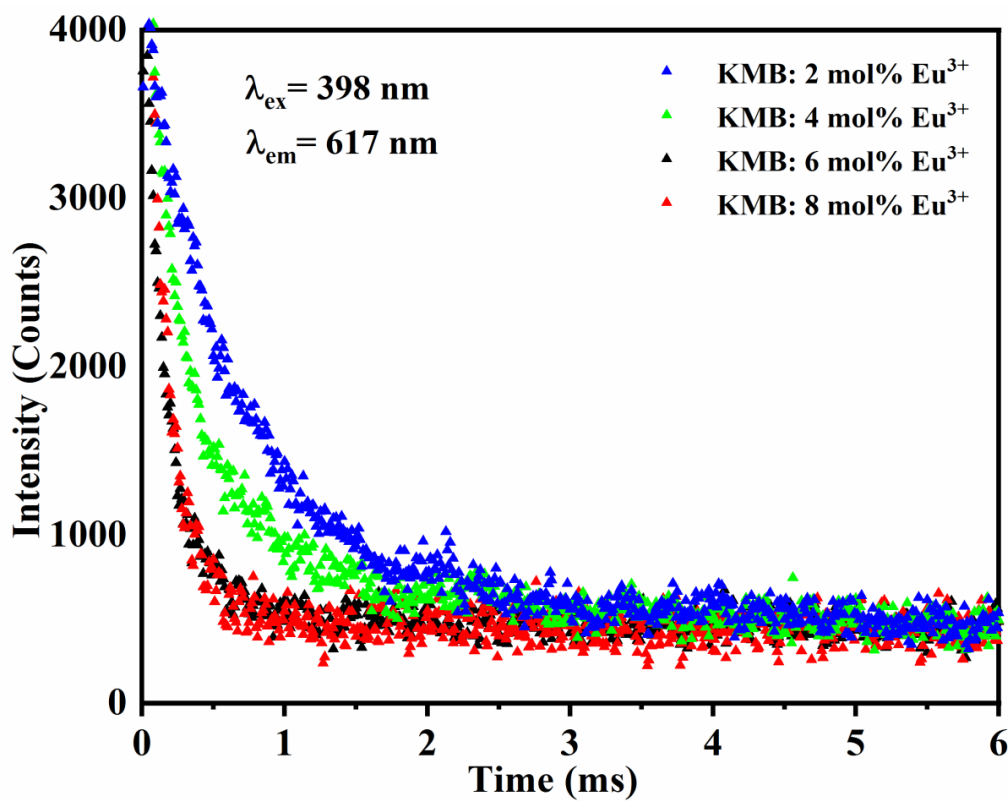


Fig. 8. Emission decay curves of  $\text{KMB: xEu}^{3+}$  ( $x = 2, 4, 6$  and  $8$  mol%) phosphors.

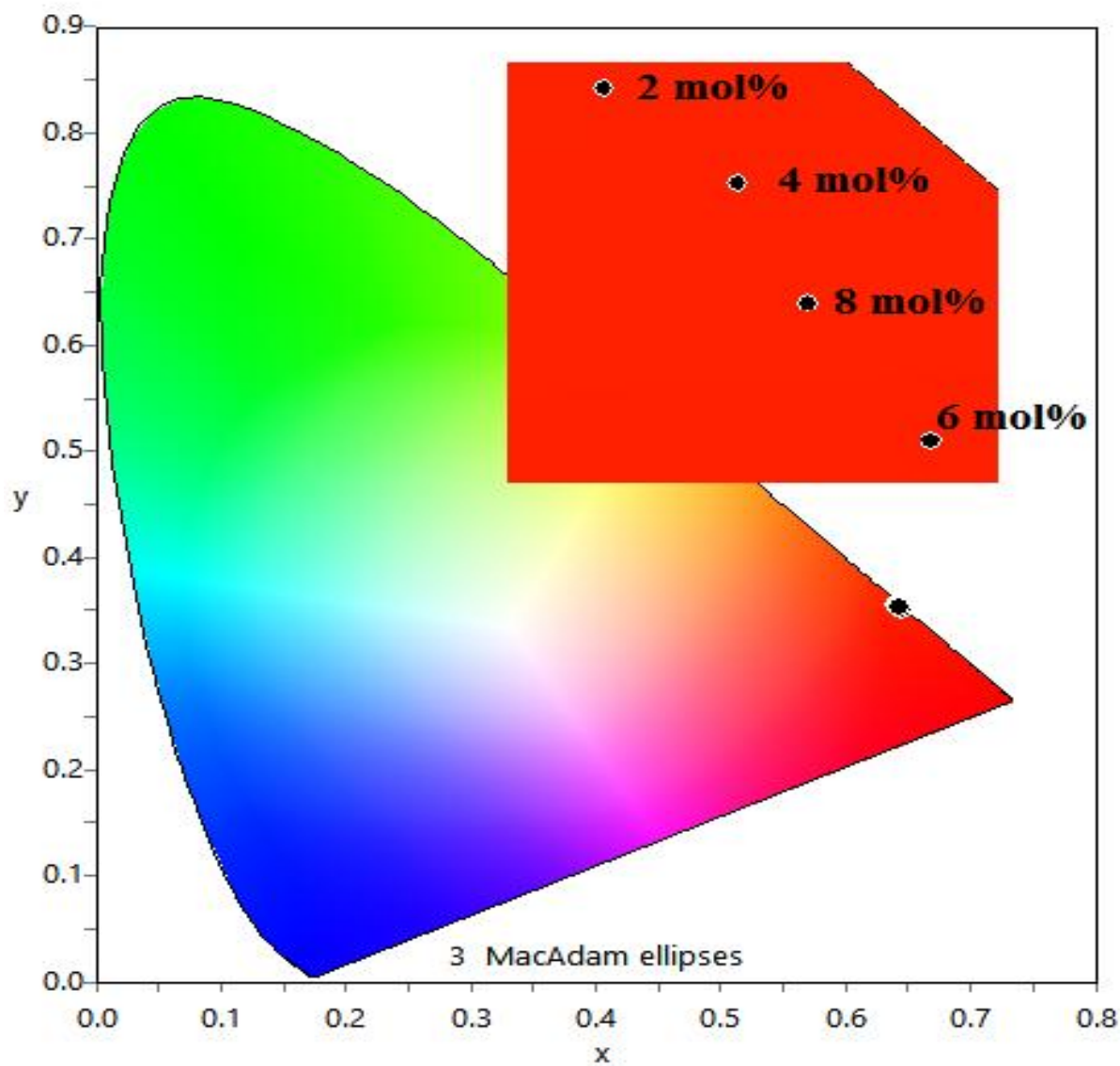


Fig. 9. CIE diagram of  $\text{KMB: xEu}^{3+}$  ( $x = 2, 4, 6$  and  $8$  mol%) phosphors.